Electronic Supporting information for the following paper:

Platinum nanoparticle decorated vertically aligned graphene screen-printed electrodes: electrochemical characterisation and exploration towards the hydrogen evolution reactions

Jessica Scremin,[1,3] Isabella V. Joviano dos Santos,[1,2] Jack P. Hughes,[1,2] Alejandro García-Miranda Ferrari,[1,2] Enrique Valderrama,[4] Wei Zheng,[4,5] Xizhou Zhong,[5] Xin Zhao,[4,5] Elen J. R. Sartori,[3] Robert D. Crapnell,[1,2] Samuel J Rowley-Neale[1,2*] and Craig E. Banks[1,2*]

[1]: *Faculty of Science and Engineering, Manchester Metropolitan University, Chester Street, Manchester M1 5GD, UK.*

[2]: *Manchester Fuel Cell Innovation Centre, Manchester Metropolitan University, Chester Street, Manchester M1 5GD, UK.*

[3]: *Departamento de Química, Centro de Ciências Exatas, Universidade Estadual de Londrina, CEP 86057-970, Londrina – PR, Brazil.*

[4]: *William and Mary Research Institute, The College of William and Mary, Jamestown Street, Williamsburg, Virginia, 23817, USA*

[5]: *Shenzhen Yick Xin Technology Development Ltd. Co., Fl. 5, Block B, Boton Technology Park, Chaguang Road, Nanshan District, Shenzhen,518055.China.*

*To whom correspondence should be addressed.

Email: S.rowley-neale@mmu.ac.uk

Email: c.banks@mmu.ac.uk; Tel: ++(0)1612471196; Fax: ++(0)1612476831

Website: www.craigbanksresearch.com

ESI Table 1. Comparison of the current literature reporting Pt based catalysts towards the Hydrogen Evolution Reaction.

Catalyst	Supporting Electrode	Stability Study (acidic media)	Deposition technique	Pt Catalyst loading	HER onset potential	Overpotential (10 mA cm^{-2})	Tafel slope (mV dec^{-1})	Reference
CNT/DenPtNPs	GC	500 cycles (+0.2 to −0.20 V) (*vs.* RHE)	Drop casting	-	− 0.016 V (*vs.* RHE)	100 mV (*vs.* RHE)	42.0	[1]
Pt-CNSs/RGO	GC	1000 cycles (+0.15 to −0.15 V) (*vs.* RHE)	Drop casting	0.17 mg cm^{-2}	− 0.018 V (*vs.* RHE)	75 mV (*vs.* RHE)	29.0	[2]
Pt NIs@f-MWCNT	GC	10000 cycles (0.00 to −0.50 V) (*vs.* RHE)	Electrochemical deposition	3.8 μg cm^{-2}	− 0.033 V (*vs.* RHE)	84 mV (*vs.* RHE)	21.2	[3]
Pt/G	GC	-	Drop cast	1 mg cm^{-2}	−0.009 V (*vs.* RHE)	25 mV (*vs.* RHE)	32.9	[4]
Pt/NG	GC	-	Drop cast	1 mg cm^{-2}	− 0.02 V (*vs.* RHE)	15 mV (*vs.* RHE)	28.4	[4]
Pt/amino-rGO	GC	200 cycles (+0.1 to −0.1 V) (*vs.* RHE)	Drop cast	5 mg cm^{-2}	− 0.02 V (*vs.* NHE)	50 mV (*vs.* RHE)	26.0	[5]
Pt/rGO	GC	200 cycles (+0.1 to −0.1 V) (*vs.* RHE)	Drop cast	5 mg cm^{-2}	− 0.03 V (*vs.* NHE)	60 mV (*vs.* RHE)	35.0	[5]
Pt/BCF	CP	1000 cycles (+0.08 to −0.40 V) (*vs.* RHE)	Spin coating	-	− 0.019 V (*vs.* RHE)	55 mV (*vs.* RHE)	32.0	[6]
Pt/WS_2	GC	1000 cycles (0.00 to −0.50 V) (*vs.* RHE)	Drop casting	4 mg cm^{-2}	− 0.04 V (*vs.* RHE)	80 mV (*vs.* RHE)	55.0	[7]
Pt atoms	Mo_2TiC_2T on carbon paper	10000 cycles (0.00 to −0.50 V) (*vs.* RHE)	Electrochemical exfoliation	1 mg cm^{-2}	− 0.03 V (*vs.* RHE)	30 mV (*vs.* RHE)	30.0	[8]
Pt@PCM	GC	5h (at -0.15 V *vs.* RHE)	Drop casting	1.5 mg cm^{-2}	− 0.02 V (*vs.* RHE)	105 mV (*vs.* RHE)	65.3	[9]
PtNi-O	GC	10h (at 10mA cm^{-2})	Drop casting	5.1 μg cm^{-2}	− 0.07 V (*vs.* RHE)	39.8 mV (*vs.* RHE)	78.8	[10]

Pt–GT–FeCo/Cu	GC	10000 cycles (0.00 to −0.30 V) (*vs.* RHE)	Drop casting	1.4 μg cm^{-2}	− 0.02 V (*vs.* RHE)	18 mV (*vs.* RHE)	24.0	[11]
PtCu RDNFs	GC	1000 cycles (0.00 to −0.50 V) (*vs.* RHE)	Drop casting	-	− 0.018 V (*vs.* RHE)	18 mV (*vs.* RHE)	35.5	[12]
PtRu@RFCS	GC	40h (at 10mA cm^{-2})	Drop casting	354 μg cm^{-2}	− 0.002 V (*vs.* RHE)	19.7 mV (*vs.* RHE)	27.2	[13]
Pt-Naf-CV	GC	4000 cycles (0.00 to −0.40 V) (*vs.* RHE	Drop casting	0.34 ug	− 0.04 V (*vs.* RHE)	34 mV (*vs.* RHE)	33.0	[14]
PC-PtN4-600	GC	10000 cycles (0.00 to −0.60 V) (*vs.* RHE)	Drop casting	364.22 μg cm^{-2}	0.00 V (*vs.* RHE)	31 mV (*vs.* RHE)	31.0	[15]
Pt SASs/AG	GC	24h (at 10mA cm^{-2})	Drop casting	7.07 mg cm^{-2}	− 0.01 V (*vs.* RHE)	12 mV (*vs.* RHE)	29.3	[16]
Pt/VG-SPE	SPE	1000 cycles (0.4 to −0.1 V) (*vs.* RHE) and 10 h at −0.1 V) (*vs.* RHE)	Screen-printed	*ca*. 4 μg cm^{-2}	− 0.003 V (*vs.* RHE)	47 mV (*vs.* RHE)	27	This Work

Key: CNH; Carbon nanohorns, PtNPs; Platinum nanoparticles, Den; Dendrimer, CNT; Carbon nanotube, CNS; Cuboid nanocrystals, RGO; reduced graphene oxide, Nis; Nano islands, MWCNTs; Multi walled carbon nanotubes, NG; Nitrogen doped graphene, amino-RGO; amine functionalized reduced graphene oxide, BCF; Bacterial cellulose derived carbon nanofibers, CP; Carbon paper, PCM; Porous carbon matrix, GT; Graphitic tubes, RDNFs; rhombic dodecahedron nanoframes, RFCS; resorcinol–formaldehyde carbon spheres, PC; Porous carbon, AG; aniline-stacked graphene, SASs; Single atoms, Pt/VG-SPE; platinum nanoparticle decorated vertically aligned graphene screen-printed electrodes, SPE; screen-printed electrode

Hydrogen Turn over frequency

Hydrogen turn over frequency (TOF) was calculated *via* the following equation:[17, 18] (for the Pt/VG-SPE).

$TOF = jS/2Fn$

where j is the measured current density at the overpotential (η) (0.01 A cm^{-2}), S is the electrochemically active surface area of the working electrode derived from the *quasi*-reversible Randles–Ševćik equation (cm^2), F is the Faraday constant, 2 is the number of electrons involved in the HER and n is the number of moles of the catalyst present in the working electrode. Note that the number of moles of Pt within the Pt/VG-SPE is calculated based on the exact loading of Pt by weight (g) on the working electrode surface, where the number of exposed active sites upon the electrode surface is not considered. Hence, it is assumed that all Pt nanoparticles on the surface of the Pt/VG-SPE are involved in the reaction.

The electroactive area of the Pt/VG-SPE was calculated using the *quasi*-reversible Randles–Ševćik equation and cyclic voltammetry (CV),[19] at different scan rates (5, 10, 15, 25, 50, 75, 100, 150, 250, and 350 mV s^{-1}):

$$i_{p^{quasi}} = \pm 0.436nFA_{real}C\left(\frac{nFDv}{RT}\right)^{\frac{1}{2}}$$

Where, i_p is the current maximum in amps (A), n is number of electrons transferred in the redox event (usually 1), F is the Faraday constant (C mol^{-1}), A_{real} is the electrochemically active surface area of the electrode (cm^2), F is the Faraday constant (C mol^{-1}), C is concentration (mol/cm^3), D is the diffusion coefficient which is 9.1×10^{-6} cm^2 s^{-1} in this case, v is scan rate (V/s), R is the gas constant (J K^{-1} mol^{-1}) and T is the temperature (298 K). The electroactive area for the Pt/VG-SPE was therefore calculated as 0.109 cm^2.

Given that the number of moles of Pt within the Pt/VG-SPE is 6.44×10^{-10} moles, the H_2 TOF value was found to be 8.77 s^{-1} for the Pt/VG-SPE.

Mass and Specific Activity

Mass activity (MA) was calculated according to the peak current (A) and the mass loading of Pt (mg) on the surface of the Pt/VG-SPE:

$$MA_{Pt} = \frac{0.0068\ A}{0.00013\ mg} = 52.31\ A\ mg^{-1}$$

Specific activity is then calculated as a function of the peak current (A) and the electroactive working area (m^2) of the Pt/VG-SPE:

$$SA_{Pt} = \frac{0.0068\ A\ mg^{-1}}{0.00109\ cm^2} = 6.24\ A\ m^{-2}$$

ESI Figure S1. Nyquist plots of Pt/VG-SPE and VG-SPEs. The electrochemical impedance spectroscopy (EIS) study was carried out under HER voltage (when each electrode reaches 10 mA cm^{-2}) in 0.5 M H_2SO_4, the frequency was from 0.1–100,000 Hz using an amplitude of 10 mV (vs. SCE). Inset: circuit utilised within experiments.

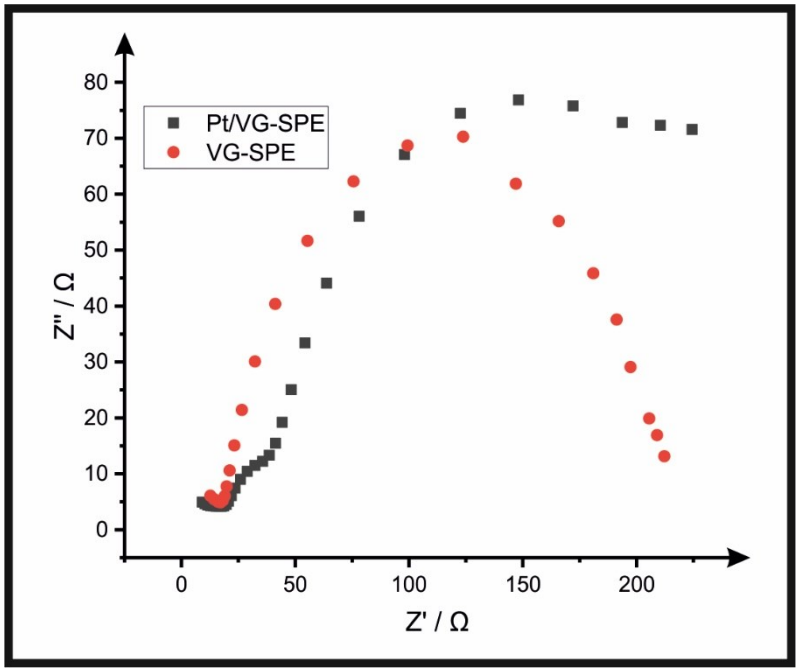

ESI Figure S2. Raman profiles and Raman mapping characterisation of the VG-SPE (A and C) and Pt/VG-SPE (D and D) respectively. Raman maps depict I_D/I_G ratios across the surface of the electrodes as a quality control measure of the batches.

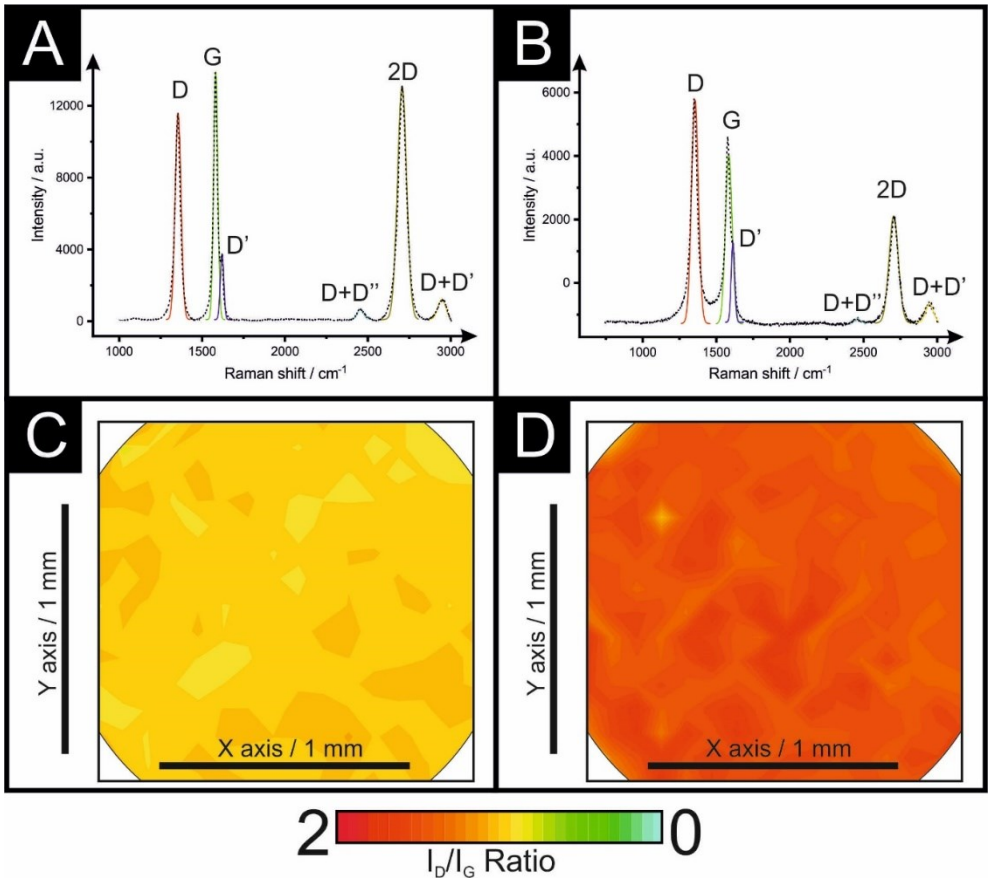

ESI Figure S3. Atomic Force Microscopy (AFM) 2D and 3D map (A and B respectively) Pt/VG-SPE sample.

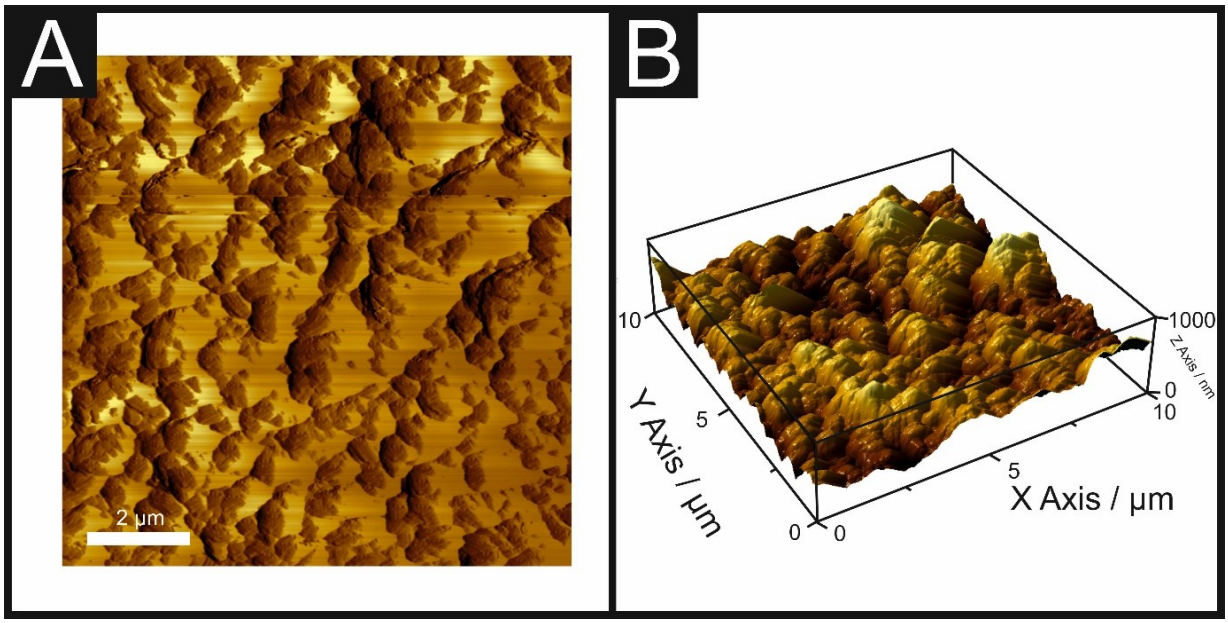

ESI Figure S4. High resolution transmission electron microscopy (HRTEM) images of the Pt/VG-SPE sample.

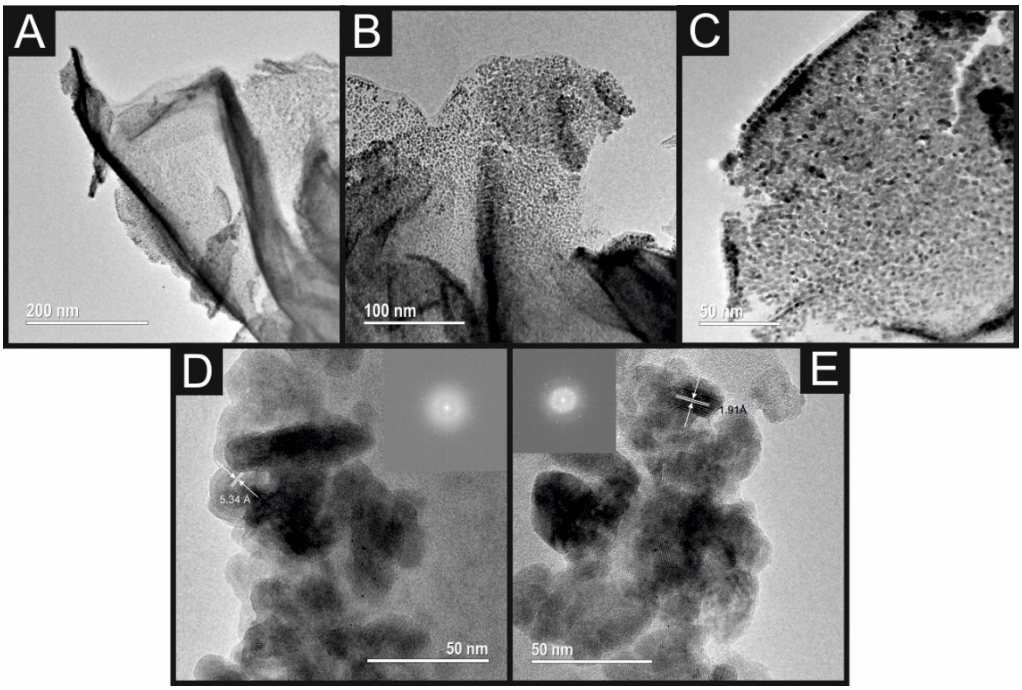

ESI Figure S5. Energy dispersive X-rays spectroscopy (EDS) analysis from the HRTEM characterisation (Figure ESI S3) of the Pt/VG-SPE sample.

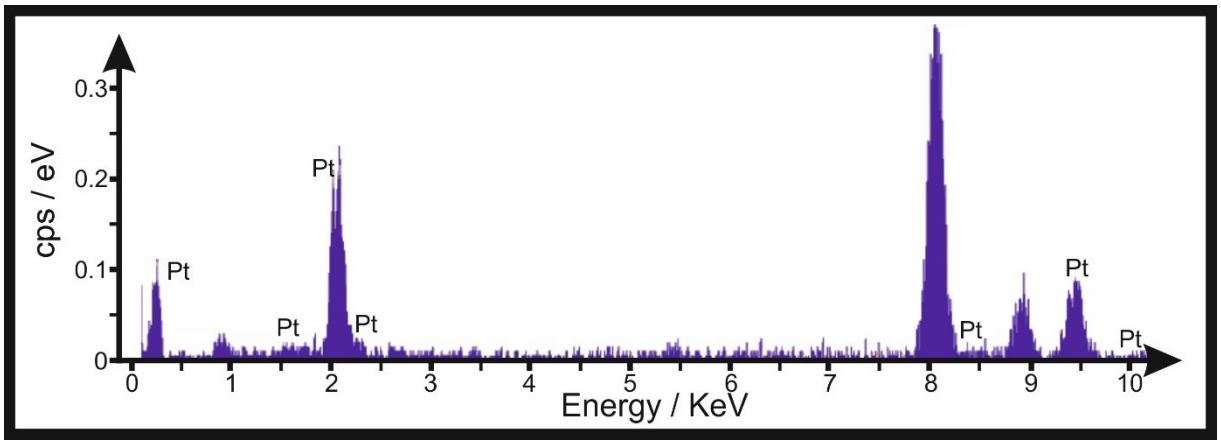

ESI Figure S6. High resolution XPS spectra for the Pt and C1s regions for the Pt/VG-SPE (A and B) and C1s region for the VG-SPE (C), respectively.

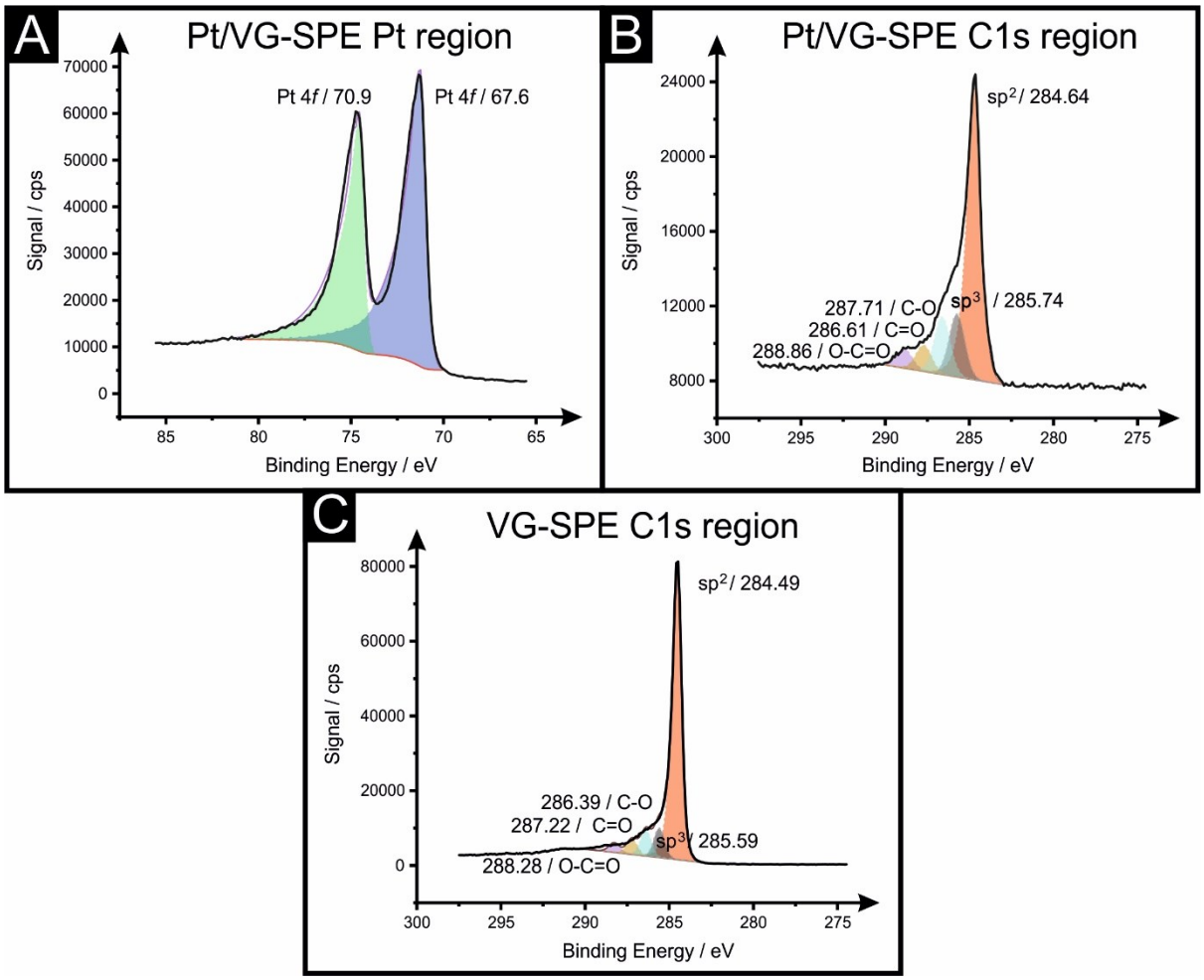

ESI Figure S7. Cyclic voltammograms recorded in 1 mM RuHex in 0.1 M KCl using VG-SPE (A) and Pt/VG-SPE (B) electrodes respectively (*vs.* SCE; 5 to 350 mV s^{-1}) at a range of voltammetric scan rates.

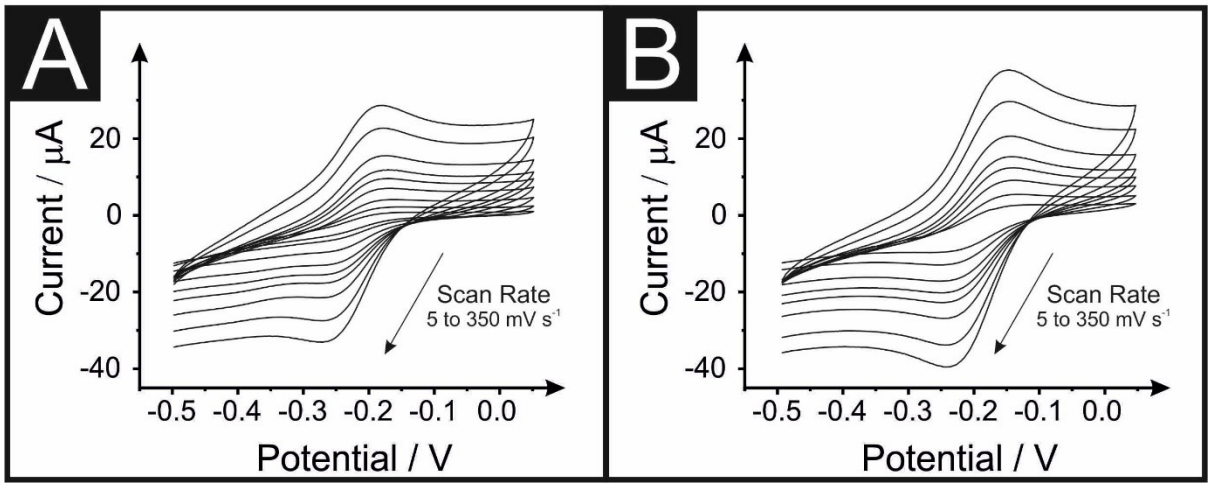

ESI Figure S8. The initial 500 seconds of the chronoamperometry scan given in Figure 4(B) using a Pt/VG-SPE for 500 seconds, Solution composition: 0.5 M H_2SO_4.

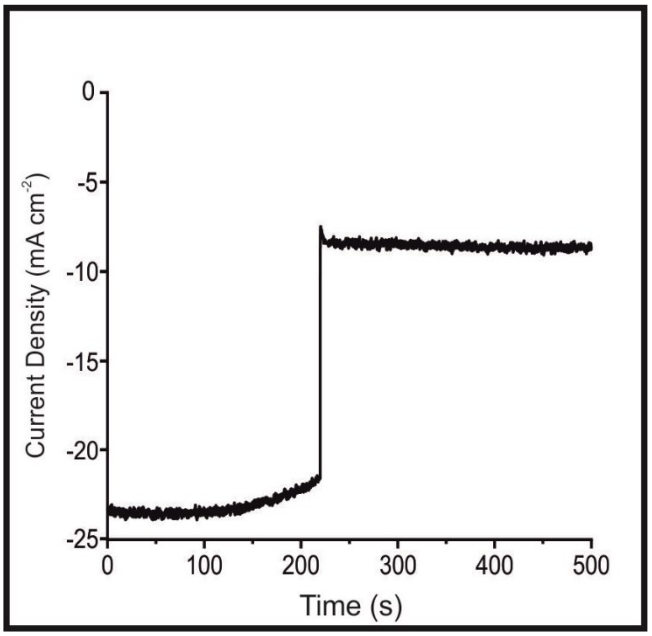

References

1. B. Devadas and T. Imae, *Electrochemistry Communications*, 2016, **72**, 135-139.
2. G.-R. Xu, J.-J. Hui, T. Huang, Y. Chen and J.-M. Lee, *J. Power Sources*, 2015, **285**, 393-399.
3. A. K. Kunhiraman, M. Ramasamy and S. Ramanathan, *Int. J. Hydrogen Energy*, 2017, **42**, 9881-9891.
4. D. Liu, L. Li and T. You, *J. Colloid Interface Sci.*, 2017, **487**, 330-335.
5. A. Navaee and A. Salimi, *Electrochim. Acta*, 2016, **211**, 322-330.
6. Y. Mi, L. Wen, Z. Wang, D. Cao, H. Zhao, Y. Zhou, F. Grote and Y. Lei, *Catal. Today*, 2016, **262**, 141-145.
7. Y. Zhang, J. Yan, X. Ren, L. Pang, H. Chen and S. Liu, *Int. J. Hydrogen Energy*, 2017, **42**, 5472-5477.
8. J. Zhang, Y. Zhao, X. Guo, C. Chen, C.-L. Dong, R.-S. Liu, C.-P. Han, Y. Li, Y. Gogotsi and G. Wang, *Nat. Catal.*, 2018, **1**, 985-992.
9. H. Zhang, P. An, W. Zhou, B. Y. Guan, P. Zhang, J. Dong and X. W. Lou, *Sci. Adv.*, 2018, **4**, 6657.
10. Z. Zhao, H. Liu, W. Gao, W. Xue, Z. Liu, J. Huang, X. Pan and Y. Huang, *J. Am. Chem. Soc.*, 2018, **140**, 9046-9050.
11. J. N. Tiwari, S. Sultan, C. W. Myung, T. Yoon, N. Li, M. Ha, A. M. Harzandi, H. J. Park, D. Y. Kim, S. S. Chandrasekaran, W. G. Lee, V. Vij, H. Kang, T. J. Shin, H. S. Shin, G. Lee, Z. Lee and K. S. Kim, *Nat. Energy*, 2018, **3**, 773-782.
12. H.-J. Niu, H.-Y. Chen, G.-L. Wen, J.-J. Feng, Q.-L. Zhang and A.-J. Wang, *J. Colloid Interface Sci.*, 2019, **539**, 525-532.
13. K. Li, Y. Li, Y. Wang, J. Ge, C. Liu and W. Xing, *Energy Environ. Sci.*, 2018, **11**, 1232-1239.
14. J. Yu, D. Wei, Z. Zheng, W. Yu, H. Shen, Y. Qu, S. Wen, Y.-U. Kwon and Y. Zhao, *J. Colloid Interface Sci.*, 2020, **566**, 505-512.
15. J. Kang, M. Wang, L. Chenbao, C. Ke, P. Liu, J. Zhu, F. Qiu and X. Zhuang, *Materials*, 2020, **13**, 1513.
16. S. Ye, F. Luo, Q. Zhang, P. Zhang, T. Xu, Q. Wang, D. He, L. Guo, Y. Zhang, C. He, X. Ouyang, M. Gu, J. Liu and X. Sun, *Energy Environ. Sci.*, 2019, **12**, 1000-1007.
17. C.-H. Kuo, I. M. Mosa, S. Thanneeru, V. Sharma, L. Zhang, S. Biswas, M. Aindow, S. Pamir Alpay, J. F. Rusling, S. L. Suib and J. He, *Chemical Communications*, 2015, **51**, 5951-5954.
18. J. P. Hughes, P. L. dos Santos, M. P. Down, C. W. Foster, J. A. Bonacin, E. M. Keefe, S. J. Rowley-Neale and C. E. Banks, *Sustainable Energy & Fuels*, 2020, **4**, 302-311.
19. A. G.-M. Ferrari, C. W. Foster, P. Kelly, D. A. C. Brownson and C. E. Banks, *Biosensors*, 2018, **8**.